Chemical Engineering Journal 204–206 (2012) 188–197

Contents lists available at SciVerse ScienceDirect

Chemical Engineering Journal

journal homepage: www.elsevier.com/locate/cej

Numerical and experimental investigation of the effects of impinging streams to enhance Ca-based sorbent capture of SO_2

Yuran Li, Fei Li, Haiying Qi *

Key Laboratory for Thermal Science and Power Engineering of Ministry of Education, Tsinghua University, Beijing 100084, China

HIGHLIGHTS

- Impinging streams significantly improve the desulfurization efficiency in a CFB reactor.
- The lateral gas flow in the impingement zone intensifies the gas–solid mass transfer.
- A method is developed to estimate the gas–solid residence time in the impingement zone.
- The residence time is significantly influenced by the gas velocity and the solid to gas mass ratio.

ARTICLE INFO

Article history:
Received 13 February 2012
Received in revised form 23 May 2012
Accepted 31 May 2012
Available online 13 June 2012

Keywords:
Desulfurization
Fluidized bed
Residence time
Solid to gas mass ratio
Mass transfer

ABSTRACT

A reactor design combining impinging streams and a circulating fluidized bed reactor (IS-CFB) was developed to improve the gas–solid mixing in fluidized beds. The Eulerian two-fluid model and a sulfation model for a CaO/fly ash sorbent were used for numerical simulations of a pilot-scale IS-CFB reactor, and the simulation results indicate that the introduction of impinging streams to a CFB reactor significantly improves the desulfurization efficiency from 89.5% to 95.1%, due to the more homogeneous radial particle volume fraction distributions and the much larger effective SO_2 capture zone. The lateral gas flow in the impingement zone intensifies the gas–solid mass transfer. Effects of the bed bulk density and the impinging particle material on the desulfurization efficiency were also investigated. Experiments were conducted using two Ca-based sorbents in a small-scale IS reactor at 750 °C. The experimental results show that the Ca/bio-based sorbent gives higher desulfurization efficiencies than the CaO/fly ash sorbent, for the latter which is large and dense cannot be effectively entrained by the impinging streams. A method for combining experiments and calculations is developed to estimate the gas–solid residence time in the impingement zone. It is found that the residence time is significantly influenced not only by the gas velocity but also by the solid to gas mass ratio.

1. Introduction

Sulfur dioxide (SO_2) in combustion flue gas is a severe problem in coal-fired power plants. A dry flue gas desulfurization (FGD) method for circulating fluidized bed (CFB) reactor has been developed for arid areas, since this technology consumes less water and has lower investment and operating costs as well as higher desulfurization efficiencies at moderate temperatures (600–800 °C). The moderate temperature desulfurization process is also promising to realize simultaneous removal of some trace heavy metals [1]. This process applied in a pilot-scale CFB reactor with a CaO/fly ash hydrated sorbent can reach a desulfurization efficiency of over 90% at a calcium to sulfur molar ratio (Ca/S) of 2.0 [2]. The desulfurization efficiency not only depends on the reaction temperature and the sorbent reactivity but also relies on the gas–solid flow structure, such as the contact efficiency and the contact residence time between the reactive gas and the sorbent particles. An internal structure and near-wall air flow were used to intensify the gas–solid mixing, for most of the sorbent particles flowed in the near-wall regions and the annular-core particle flow structure also made the sorbent particles concentrate in the near-wall regions, which decreased the gas–solid contact efficiency [2–4].

Due to the excellent mixing of the two phases, impinging streams (ISs) are always of interest. Impinging streams involve two streams entering the impingement zone through two closely spaced inlets along the same axis in opposing directions. Simultaneously, the particles are carried by the IS into the impingement zone, and will be carried away from the impingement zone after a few times oscillation. Owing to the fast and unsteady motion, the mean particle residence time in the impingement zone is greatly prolonged, and the violent interaction accordingly enhances the heat and mass transfer processes [5]. Impinging stream designs recently have many applications in chemical reactors and

* Corresponding author. Tel./fax: +86 10 62796036.
E-mail address: hyqi@mail.tsinghua.edu.cn (H. Qi).

1385-8947/$ - see front matter © 2012 Elsevier B.V. All rights reserved.
http://dx.doi.org/10.1016/j.cej.2012.05.115

Nomenclature

C_{SO_2}	SO_2 concentration, dimensionless
d_s	particle diameter, μm
D_{SO_2}	SO_2 diffusion coefficient, m^2/s
M_{CaO}	CaO molecular weight, mg/mol
M_{CaSO_4}	$CaSO_4$ molecular weight, mg/mol
n	exponent of the SO_2 concentration, dimensionless
p	gas phase pressure, Pa
p_s	solid phase pressure, Pa
r_X	desulfurization reaction rate, s^{-1}
S	desulfurization reaction source term
$[SO_2]$	SO_2 concentration, ppm
t	reaction time, min
t_f	residence time for the particles in the upper part of the furnace, s
t_{is}	residence time for the particles in the impingement zone, s
T	reaction temperature, K
T_{is}	temperature in the impingement zone, °C
u	velocity, m/s
U	gas velocity in the furnace, m/s
U_{is}	gas velocity in the impinging stream inlets, m/s
V	volumetric gas flow rate at standard state, L/min
x	reactor diameter, m
X	calcium conversion rate, dimensionless
y	reactor height, m
y_{CaO}	CaO mass fraction in the sorbent, dimensionless
Y_{SO_2}	SO_2 mass fraction, dimensionless

Greek symbols

α	impinging stream ratio, dimensionless
β	drag coefficient between gas and solid phases, $N\,s/m^4$
ε	volume fraction, dimensionless
η	desulfurization efficiency, dimensionless
λ	bulk viscosity, Pa s
μ	shear viscosity, Pa s
ξ_a	attrition friction,%
ρ	density, kg/m^3
$\bar{\bar{\tau}}$	shear stress, Pa

Subscript

f	furnace
g	gas
is	impinging streams
s	solid

mixers and in wet FGD of coal-fired power plant exhaust [6–8]. Berman et al. [9,10] studied the SO_2 absorption with a $Ca(OH)_2$ water suspension in an IS reactor, in which the desulfurization efficiency was 94–97% at Ca/S = 1.8. In another gas-continuous IS gas–liquid reactor, the desulfurization efficiency reached 91.8% with a $Ca(OH)_2$ water suspension at Ca/S = 1.4 [11]. The particle residence time in the impingement zone is difficult to measure, since this zone has no physical boundaries and the particles are dispersed. Radioactive particles as tracers and Monte Carlo simulation have been used to study the particle residence time, which was estimated to be about 1.0 s or less [12–14].

Two kinds of Ca-based sorbent, a CaO/fly ash hydrated sorbent and a Ca/bio-based sorbent were used in this work. The CaO/fly ash hydrated sorbent had been developed for many years and used for low-temperature and moderate-temperature FGD, for the sorbent had a coarse and porous composite structure with fine calcium-containing materials adhered on larger fly ash surfaces [15–18]. The Ca/bio-based sorbent prepared from a mixture of lime and biomass was used for SO_2 capture due to its light weight and the biomass was utilized as a dispersion medium to increase the surface area and pore volume of the sorbents [19,20]. The advantages of the IS lead to the conceptual design of an IS-CFB reactor combining impinging streams and a circulating fluidized bed reactor for use with the Ca-based sorbents to capture SO_2. The numerical simulation predictions for a CFB reactor agreed well with the experimental results which were generated from a pilot-scale CFB reactor [21,22]; therefore, numerical simulations were also used to predict the mixing behavior in the IS-CFB reactor. To reduce the influence of the particle circulating ratio and to greatly reduce the required amount of sorbent, a small-scale IS reactor was developed to verify the enhancement effect of the IS on the desulfurization efficiency.

2. Numerical and experimental conditions

2.1. Geometrical model and numerical conditions for a concept IS-CFB reactor

The concept reactor combining IS and a CFB reactor (IS-CFB) is shown schematically in Fig. 1, and the reactor size was based on an actual pilot-scale CFB reactor with a 6.0 m height and a 0.305 m diameter. The flue gas carrying the spent sorbent particles was injected into the bed to generate impinging streams in the central zone of the reactor. These then began to fluidize upward in the bed. The inlet diameter for the impinging stream was 80 mm. The ratio of the fresh sorbent feed rate to the gas flow rate was designed to satisfy Ca/S = 2.0 [2,21]. The ratio of the gas flow rate used in the impinging streams to the total gas flow rate was defined as the impinging stream ratio, α. The inlet SO_2 concentration in the fresh flue gas was 1500 ppm. The bed bulk density (inventory) was 33.3 kg/m^3 and the operating temperature was 750 °C. The bed superficial gas velocity was 2.5 m/s, of which part was used to generate the impinging streams. A CaO/fly ash hy-

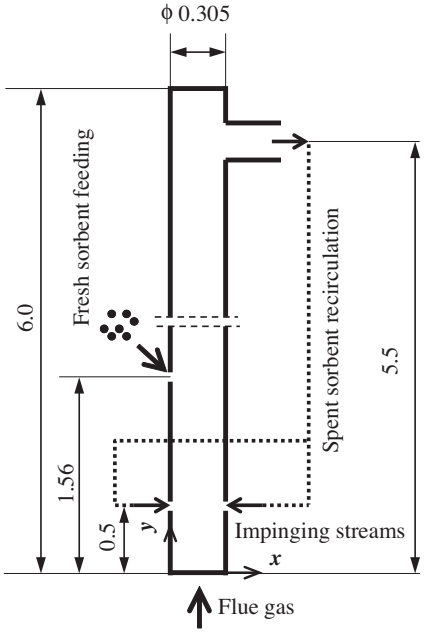

Fig. 1. IS-CFB reactor structure schematic diagram (Unit: m).

Table 1
Material properties.

Gas density	Gas viscosity	Particle diameter	Sorbent density
ρ_g (kg/m^3)	μ_g (Pa s)	d_s (μm)	ρ_s (kg/m^3)
0.362	41.77×10^{-6}	83	1000

Table 2
Gas flow rate operating conditions.

V (L/min)	U (m/s)	U_{is} (m/s)	t_f (s)	T_{is}(±5 °C)
27.7	0.75	18.60	0.80	680
31.7	0.85	21.29	0.70	665
35.6	0.96	23.91	0.63	650
39.6	1.07	26.59	0.56	630

drated sorbent was used and the physical properties are listed in Table 1.

The Eulerian two-fluid model and a sulfation model for the CaO/fly ash sorbent were used to predict the particle volume fraction and SO_2 distributions in the riser of a two-dimensional CFB reactor. Gas turbulence was neglected for its effect was limited in comparison with gas–solid interactions in dense flows in CFB reactors [23,24]. The simulations were verified with experimental results from CFB riser tests [18,22]. The model equations are:

Continuity equation:

$$\frac{\partial}{\partial t}(\varepsilon_k \rho_k) + \nabla \cdot \left(\varepsilon_k \rho_k \vec{u}_k\right) = S_k, \ k = g, s \tag{1}$$

$$\varepsilon_g + \varepsilon_s = 1 \tag{2}$$

$$S_s = -S_g = \rho_s \varepsilon_s y_{CaO} \frac{M_{CaSO_4} - M_{CaO}}{M_{CaO}} r_X \tag{3}$$

where subscript g means gas phase and s means solid phase, ε_k is the k phase volume fraction, ρ_k is the density, u_k is the k phase velocity, S_k is the source term due to the desulfurization reaction, and y_{CaO} is the CaO mass fraction in the sorbent. M_{CaO} is the molecular weight of the reactant CaO and M_{CaSO_4} is the molecular weight of the product $CaSO_4$. r_X is the desulfurization reaction rate based on the calcium conversion rate.

Momentum equation:

$$\frac{\partial}{\partial t}(\varepsilon_g \rho_g \vec{u}_g) + \nabla \cdot (\varepsilon_g \rho_g \vec{u}_g \vec{u}_g) = -\varepsilon_g \nabla p + \nabla \cdot \bar{\bar{\tau}}_g + \varepsilon_g \rho_g \vec{g} - \beta(\vec{u}_g - \vec{u}_s) \tag{4}$$

$$\frac{\partial}{\partial t}(\varepsilon_s \rho_s \vec{u}_s) + \nabla \cdot (\varepsilon_s \rho_s \vec{u}_s \vec{u}_s) = -\varepsilon_s \nabla p - \nabla p_s + \nabla \cdot \bar{\bar{\tau}}_s + \varepsilon_s \rho_s \vec{g} + \beta(\vec{u}_g - \vec{u}_s) \tag{5}$$

where p and p_s are the gas and solid phase pressures, $\bar{\bar{\tau}}$ is the shear stress:

$$\bar{\bar{\tau}}_k = \varepsilon_k \mu_k \left[\nabla \vec{u}_i + (\nabla \vec{u}_i)^T\right] + \varepsilon_k \left(\lambda_k - \frac{2}{3}\mu_k\right) \nabla \cdot u_k \bar{\bar{I}}, \ k = g, s \tag{6}$$

where, the solid phase bulk and shear viscosities, λ_s and μ_s are determined with the Kinetic Theory of Granular Flows (KTGFs) [25]. β is the momentum exchange coefficient (drag coefficient) between the gas phase and the solid phase, calculated from the QL-EMMS (Qi/Li-Energy Minimization Multi Scale) model [26].

SO_2 species equation:

$$\frac{\partial}{\partial t}(\varepsilon_g \rho_g Y_{SO_2}) + \nabla \cdot (\varepsilon_g \rho_g Y_{SO_2} \vec{u}_g) = -\varepsilon_g \rho_g D_{SO_2} \nabla Y_{SO_2} - \rho_s \varepsilon_s x_{CaO} \frac{M_{SO_2}}{M_{CaO}} r_X \tag{7}$$

where Y_{SO_2} is the mass fraction and D_{SO_2} is the diffusion coefficient for SO_2 with a value of 2.88×10^{-5} m^2/s.

Calcium conversion equation:

$$\frac{\partial}{\partial t}(\rho_s \varepsilon_s X) + \nabla \cdot (\rho_s \varepsilon_s \vec{u}_s X) = \rho_s \varepsilon_s r_X \tag{8}$$

where X is the calcium conversion rate. r_X for the CaO/fly ash hydrated sorbent sulfation model [18] is expressed as:

$$r_X = k(T) \cdot g(X) \cdot C_{SO_2}^n \tag{9}$$

where T = 1023 K, $C_{SO_2} = 1500$ ppm. The parameter, n, is the exponent of the SO_2 concentration equal to 0.88 since the reaction is in the rapid reaction stage ($X \leqslant 0.5$ for Ca/S = 2.0). These equations were solved using the commercial software FLUENT 6.3.26. The source terms due to the desulfurization reaction, the drag coefficient between the gas and solid phases and the calcium conversion reaction were implemented with FLUENT UDF functions.

During the simulations, particles escaping from the top outlet were sent back to the riser via the impinging stream inlets to maintain a constant inventory in the riser. The calcium conversion at the

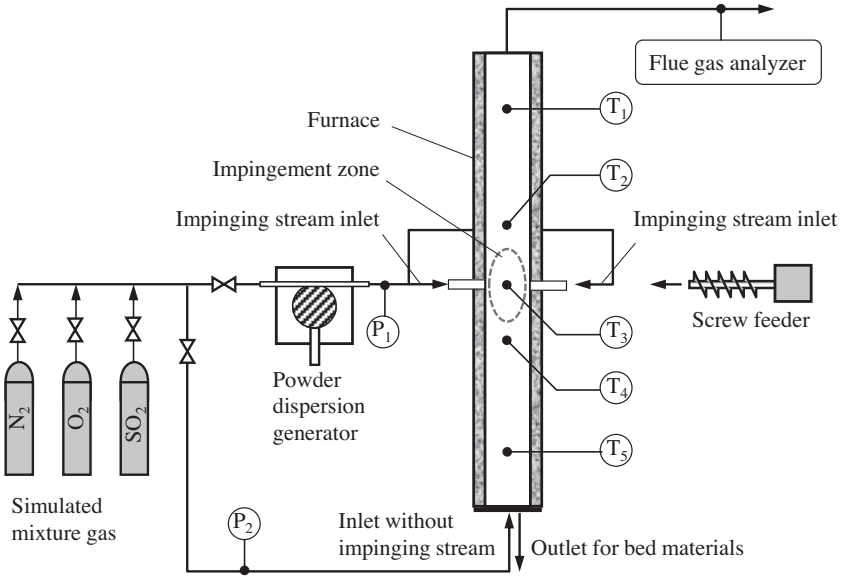

Fig. 2. Impinging stream reactor experimental system diagram.

Table 3
Chemical compositions of the lime, fly ash and biomass ash (%).

	SiO_2	Al_2O_3	Fe_2O_3	CaO	MgO	K_2O	Na_2O	P_2O_5	TiO_2	SO_3	Ignition loss
Lime	3.64	0.34	0.44	86.45	3.51	1.01	0.05	0.11	0.013	–	4.39
Fly ash	48.45	36.64	5.12	2.86	1.02	1.01	0.44	0.50	1.27	–	2.69
Biomass ash	51.08	9.72	4.74	14.84	3.72	6.45	2.10	1.34	0.44	1.32	4.25

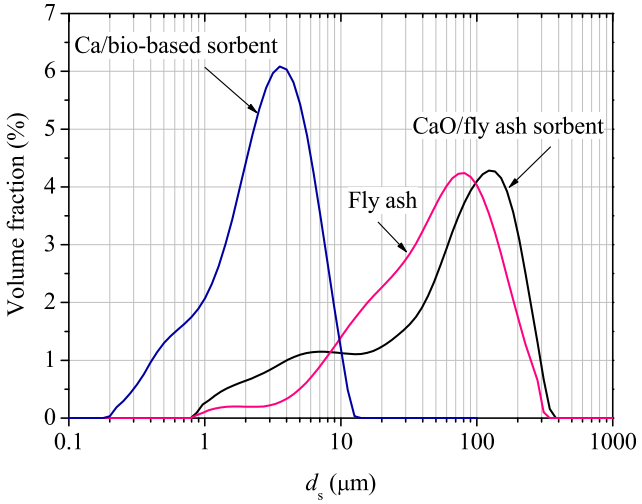

Fig. 3. Fly ash and the Ca-based sorbent particle size distributions.

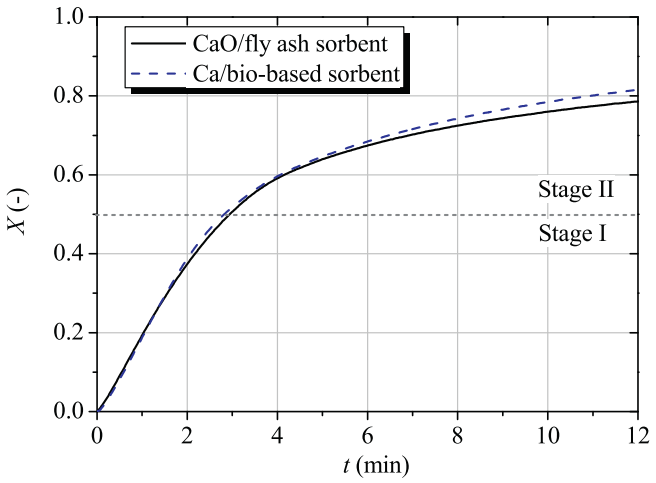

Fig. 4. Calcium conversion rates for the two sorbents.

Table 4
Specific weights of the CaO/fly ash sorbent and the Ca/bio-based sorbent.

Sorbent	Weight loss at 750 °C (%)	Mass fraction of CaO (%)	Sorbent weight at ambient temperature (kg/kg CaO)	Loading density (kg/m^3)
CaO/fly ash sorbent	6	19.6	5.43	1000
Ca/bio-based sorbent	24	84.3	1.56	310

impinging stream inlets was set equal to the value at the top outlet to simulate the real solid circulation. The pressure at the riser outlet was set equal to the atmospheric pressure with all the gradients of the other variables set to zero at the outlet. No slip velocity wall conditions were used for both phases. A $15 \times 58 \times 1$ orthogonal grid was used for the computational domain with local grid refinement applied near the bed walls. The transient analysis used a 0.001 s time step to simulate the gas–solid two-phase flow and the desulfurization reaction. The flow was first simulated without reactions, and then the reaction model was included after the flow became steady. A previous study showed that the predicted riser pressure drop and desulfurization efficiency agreed well experimental data, with relative errors of −2.96% and 5.68%. Those results proved the accuracy of the two-phase model as well as the sulfation model [22]. This work predicts the two-phase flow and desulfurization in the IS-CFB reactor. Results are given for the effects of various variables including the impinging stream ratio, bed bulk density, impinging stream velocity and impinging particle material on the desulfurization efficiency.

2.2. An IS reactor experimental setup

The experiments were conducted in a small size IS reactor. The experimental system shown in Fig. 2 consisted of an 8 kW heating furnace (custom-made), a stainless steel reactor (custom-made) 1200 mm in high and 52 mm in diameter, a powder dispersion generator (PALAS, RBG-2000), a screw feeder (VTV, YN70-20C), a flue gas analyzer (RBR, ecom-J2KN) and simulated mixture gas. The desulfurization efficiencies with and without IS were studied using three midlevel inlets at 600 mm height and one bottom inlet, each with a 7 mm diameter. The third midlevel inlet was perpendicular to the diameter connecting the other two which produced strongly interacting streams.

To generate impinging streams, the sorbent particles generated by the powder dispersion generator were carried by the flue gas to the two opposing inlets, and the flue gas was all delivered through the two jets. For the flow without IS, the screw feeder supplied the sorbent particles to the third middle inlet, and the flue gas was all input though the bottom inlet. The powder dispersion generator and screw feeder controlled the sorbent supply rate (error of 3%) while the mass flow controller measured the gas flow rate (error of 2%). The gas and solid flow rates through the two opposing inlets were equal. The total gas–solid flow rates were equal with and without IS.

The design operating temperature was 750 °C (error of ±5 °C). The gas flow rate at standard state, V, and gas operating conditions are listed in Table 2, where U is the gas velocity in the furnace and U_{is} is the impinging stream velocity. If a large gas flow rate is used, the bag filter cannot effectively collect particles. As the volumetric flow rate increased, the residence time, t_f, for the gas in the upper furnace and the temperature, T_{is}, in the impingement zone both decreased, while the other four test temperatures as shown in Fig. 2 stayed at 750 °C. Conversely, for the pilot-scale CFB reactor, when the gas velocity increased T_{is} kept constant due to the flue gas from an oil burner. The design inlet SO_2 concentration was 1500 ppm. The outlet SO_2 concentrations were measured by the flue gas analyzer. The desulfurization efficiency, η, was calculated from the ratio of the difference between the inlet and outlet SO_2 concentrations to the inlet SO_2 concentration. The flue gas analyzer measurement error ranged from 10 to 20 ppm. The experimental error on the desulfurization efficiency ranged from 3% to 5%.

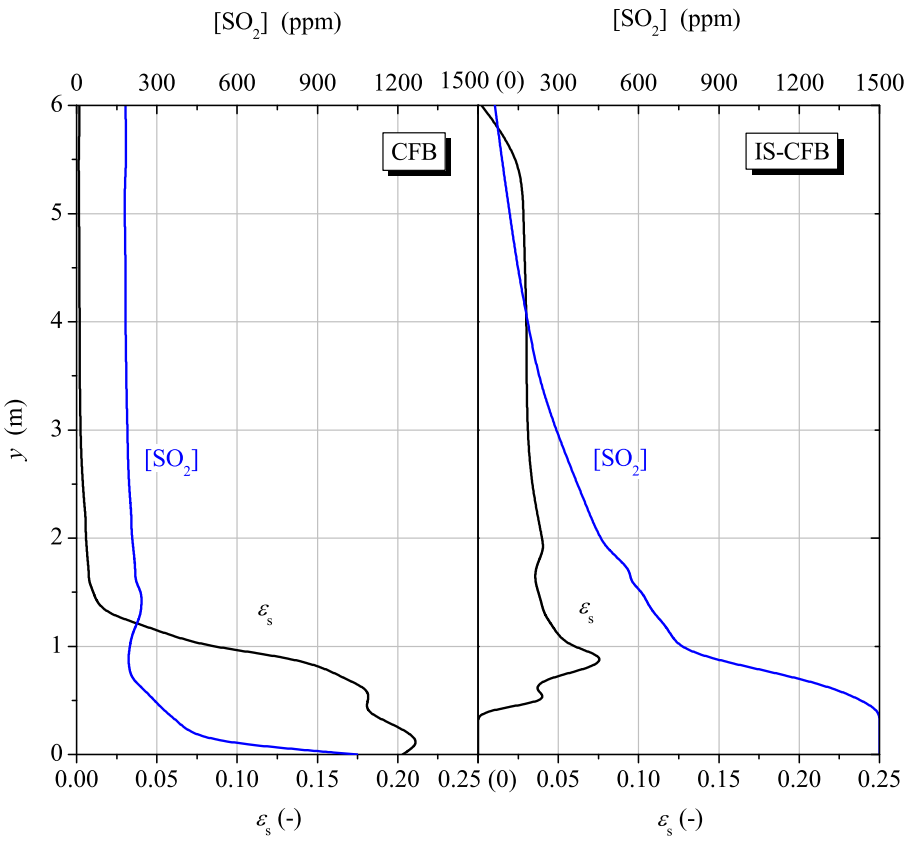

Fig. 5. Simulated SO_2 concentrations and particle volume fraction distributions averaged over each cross section (α = 20% for the IS-CFB reactor).

2.3. Ca-based sorbent

Experiments have been conducted using the CaO/fly ash sorbent to capture SO_2 in a pilot-scale CFB reactor and a sulfation model for the CaO/fly ash sorbent has been developed [18,21]; therefore, the CaO/fly ash sorbent is used in the concept IS-CFB reactor for numerical simulations. When the CaO/fly ash sorbent is injected into the IS reactor the desulfurization efficiency decreases. Accordingly, a Ca/bio-based sorbent with light weight is developed to verify the enhancement effects of impinging streams on the desulfurization efficiency.

The lime was from the Shougang Building Materials Chemical Plant, the fly ash was from the Beijing Shijingshan Power Plant, and the biomass (sawdust) was from the Daxing District, Beijing. Their chemical compositions measured by an ARL ADVANT XP+type X-ray fluorescence spectrometer are listed in Table 3. The lime particles were crushed to less than 20 mm in size. The fly ash particle size distribution measured by a Malvern Mastersizer 2000 was shown in Fig. 3 with a volume mean particle diameter of about 75 μm. The lime and fly ash were slurried together with water for 1 h with a lime to fly ash mass ratio of 1:4. The slurry was then filtered through a vacuum filter to form a filter cake. Then, the filter cake was dried in an infrared desiccator to produce the CaO/fly ash sorbent powder holding less than 10% water with a volume mean particle diameter of about 120 μm. The Ca/bio-based sorbent was prepared from lime and sawdust. After comparison of the effects of different size particles, the sawdust was sieved to 0.5–1.0 mm particles. The lime and sawdust were both immersed in water with a lime to biomass mass ratio of 9:1. Then the biomass slurry and the lime slurry were blended together. The slurry was agitated for 30 min and then filtered through a vacuum filter to make a semi-dry filter cake. Then, the filter cake was dried in an infrared desiccator to form a dry sorbent cake with a water content of less than 5%. The drying time was 0.5–1.0 h for drying temperatures of 150 °C. The sorbent cakes were crushed and sieved to fine particles for use in the IS reactor. All the particles were less than 15.0 μm in size, with a volume mean particle diameter of about 3.5 μm as shown in Fig. 3.

The sorbent weight at ambient temperature per kilogram CaO was defined as the specific weight calculated based on the weight loss and the CaO fraction. As the biomass was heated to 750 °C in N_2 in a thermogravimetric analyzer (TGA, TA Q500), the biomass began to decompose at 240 °C and was completely calcined to biomass ash at 750 °C. As the two sorbents were heated to 750 °C in N_2, the weight losses were shown in Table 4. After calcinations, the CaO fractions in the sorbents were calculated, and then the specific weights were obtained as shown in Table 4. The fly ash loading density was about 1200 kg/m^3 and the fly ash mass fraction in the sorbent was about 80%; therefore, the loading density of the CaO/fly ash sorbent was about 1000 kg/m^3 larger than the Ca/bio-based sorbent of about 310 kg/m^3. The two sorbents had approximately equal calcium conversion rates, which were measured in the TGA with an equal CaO mass, as shown in Fig. 4. The composition of the reactive gas was fixed at 1 vol.% SO_2, 5 vol.% O_2, and the balance gas being N_2. The reactive gas was admitted to start the run at 750 °C. The dry gas flow rate at ambient conditions was 100 ml/min.

3. Results and discussion

3.1. Numerical simulations

3.1.1. Enhancement effects of impinging streams on the CFB reactor

The axial distributions of the SO_2 concentration, [SO_2], and the particle volume fraction, ε_s, averaged over each cross section are

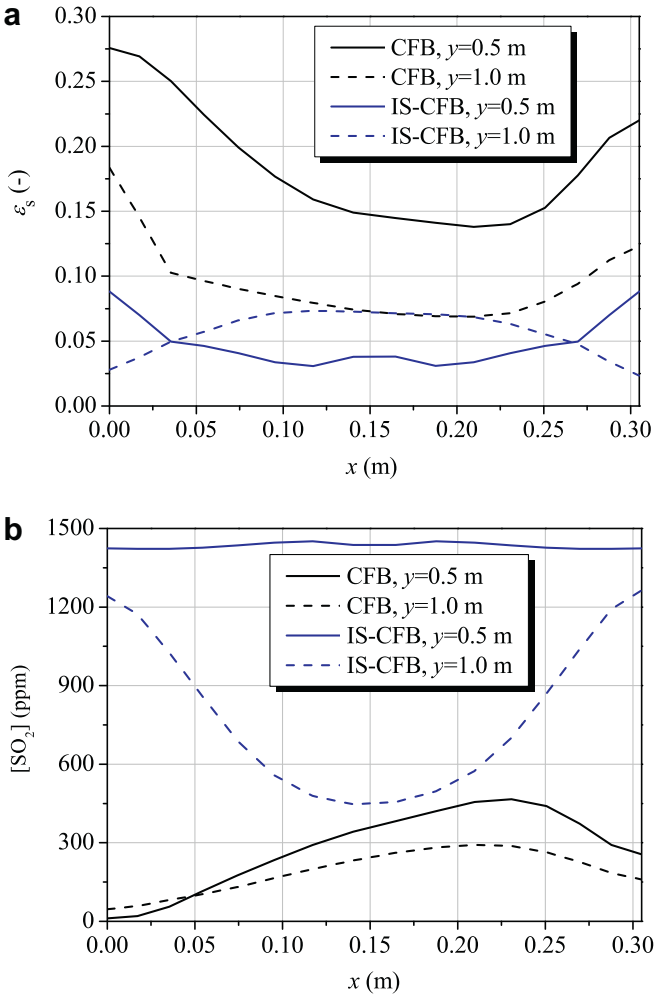

Fig. 6. Radial particle volume fraction (a) and SO_2 concentration (b) distributions (α = 20% for the IS-CFB reactor).

shown in Fig. 5. The particle volume fraction distribution is much more homogeneous in the IS-CFB reactor for the highest particle volume fraction is much lower than in the CFB reactor, which indicates the effectiveness of the gas–solid mixing. The outlet SO_2 concentration for the IS-CFB reactor is 74 ppm less than the 158 ppm for the CFB reactor. Thus, the desulfurization efficiency is increased from 89.5% to 95.1%. The desulfurization efficiency of 89.5% in the CFB reactor was verified by experimental results in a CFB reactor [22]. The effective SO_2 capture zone in the IS-CFB reactor is much longer than in the CFB reactor. For the IS-CFB reactor, the particle volume fraction is relatively homogeneous in the zone from 0.5 m to 5.5 m. For the CFB reactor, almost all the sorbent particles gather together in the zone from 0 m to 1.5 m, where the SO_2 concentration decreases from 1500 ppm to 200 ppm. Above the 1.5 m height, the SO_2 concentration changes very little since the particle volume fraction is near zero. For the IS-CFB reactor, the SO_2 concentration distribution decreases from 1450 ppm to 450 ppm from 0.5 m to 1.0 m height, which means 50% SO_2 is removed in this 0.5 m with a relatively small amount of sorbent, compared to the very limited SO_2 reduction in the same section of the CFB reactor with more sorbent.

The radial distributions for the particle volume fraction and the SO_2 concentration at the 0.5 m and 1.0 m heights in the two reactors are shown in Fig. 6. At the 0.5 m height, the particle volume fraction in the IS-CFB reactor is low in the center and much high near the wall, with the same trend found in the CFB reactor. The profiles of the particle volume fraction distribution were consistent with previous pilot-scale experimental results [27]. At the 1.0 m height, the shape of the particle volume fraction distribution for the IS-CFB reactor is the opposite of the 'core-annular' structure in the traditional CFB reactor, with the SO_2 concentration higher in the center and approaching zero near the wall. Thus the impinging streams improve the particle volume fraction distribution and homogeneity of the gas–solid phase; therefore, the mass transfer coefficient and gas–solid reaction rate are also increased.

The gas velocity field in a vertical center plane is shown in Fig. 7. In the impingement zone, the lateral gas flow is very strong as the gas flow impinges the opposing jet flows, which improves the gas–solid mass transfer. The axial gas velocity distribution in the cross section of the IS-CFB reactor is more homogeneous than for the conventional CFB reactor, as shown in the square. The flow fields above the impingement zone for both reactors are similar with little lateral gas flow movement. The axial gas velocity is low near the wall and higher in the central zone.

The impinging streams have been shown to significantly improve the desulfurization efficiency, while this effect has been still underestimated in the numerical simulations. The particles expose fresh surface to the reactive gas and the mass transfer coefficient increase, which is not considered for the IS-CFB reactor, leading to a low desulfurization efficiency.

3.1.2. Effects of impinging stream parameters and impinging particle materials on the desulfurization efficiency

The impinging stream parameters were then optimized to maximize the desulfurization efficiency and minimize the bed pressure drop. The impinging stream ratio, α, and the bed bulk density, ρ_{bed}, were varied individually in simulations while all the other parameters were held constant. Fig. 8 shows that, when increasing α from 10% to 50%, the desulfurization efficiency increases initially and reaches the maximum between α = 20–40%, and then decreases. The desulfurization efficiency increases continuously with increasing bed bulk density, which means that more sorbent improves the desulfurization. The figure also shows that even a bed bulk density of only 3/4 (25 kg/m^3) that of the CFB reactor (33.3 kg/m^3) gives a much high desulfurization efficiency in the IS-CFB (93%). Since the bed bulk density is proportional to the bed pressure drop, the IS-CFB reactor gives a much higher desulfurization efficiency with a much lower bed pressure drop than the CFB reactor.

The impinging particle material (fresh sorbent or circulating spent sorbent) is very important for the desulfurization process in the IS-CFB reactor. The impinging velocity, U_{is}, is also very important in the IS reactor. The effects of these two parameters on the desulfurization efficiency are investigated. To produce a higher U_{is} with the same flow rate, the IS inlet diameter was reduced from 80 mm to 10 mm. The increasing velocity creates a lower inlet particle concentration. Therefore, the inlet particle concentration was set to ε_{is} = 0.02 to be more realistic. The impinging stream ratio (α = 40%) and bed bulk density (ρ_{bed} = 33.3 kg/m^3) were hold constant. When the fresh sorbent was used, the circulating spent sorbent was still sent back to the reactor to the circulating inlet of the CFB reactor.

Table 5 shows that the desulfurization efficiency decreases from 95.0% to 93.4% as the impinging stream velocity increases, and is still higher than the desulfurization efficiency in the CFB reactor (89.5%). The desulfurization efficiency is lower for the fresh sorbent than the circulating spent sorbent. The calcium conversion of the spent sorbent entering the reactor is about 50% while the calcium conversion of the fresh sorbent is 0. Thus, according to the sulfation model [18], the reaction rate of the fresh sorbent is about 5 times that of the spent sorbent; however, the flow rate of the circulating spent sorbent is about 100 times that of the fresh sorbent, and the

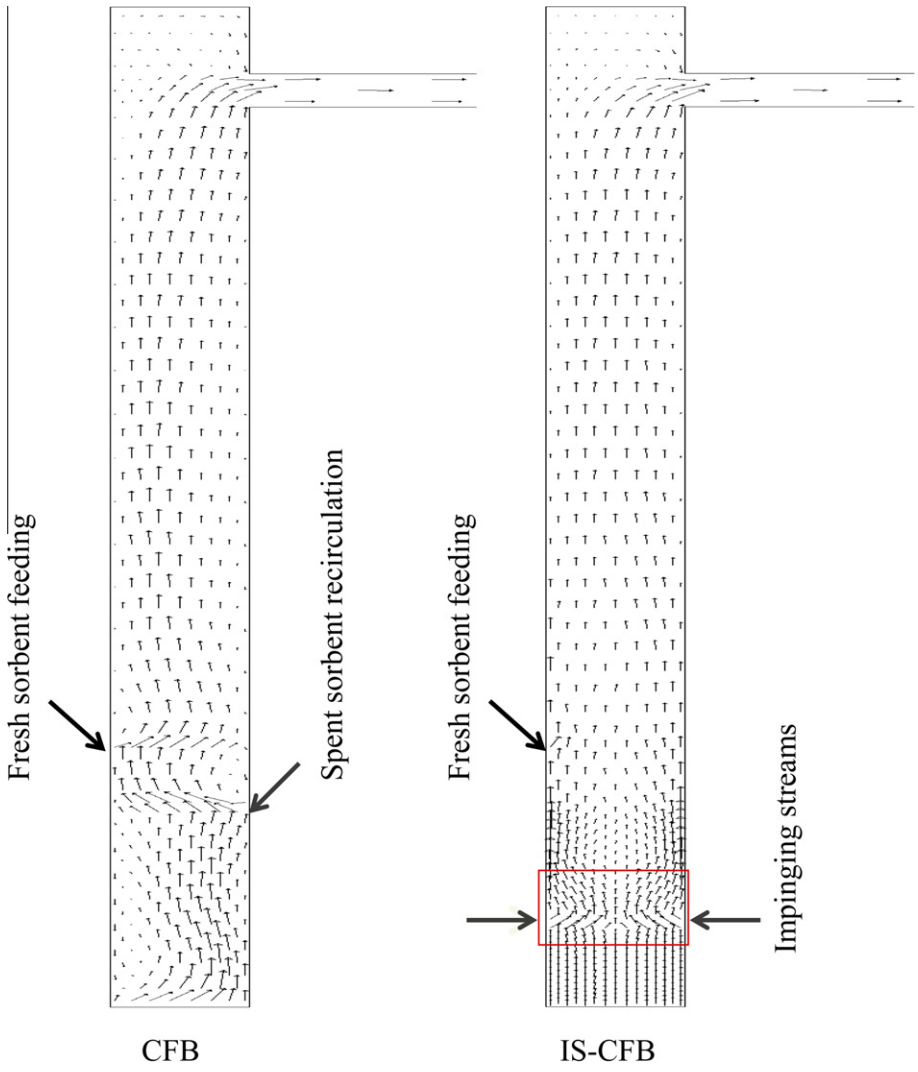

Fig. 7. Gas velocity distribution in the vertical center plane (α = 20% for the IS-CFB reactor).

spent sorbent is easily broken into pieces by the impinging particles, which exposes more surface to the reactive gas. The total desulfurization capacity of the recirculation spent sorbent is then higher than that of just circulating fresh sorbent once through the reactor. The spent sorbent can then be fully used in the process.

3.2. Experimental verification

3.2.1. Effects of impinging streams on the desulfurization efficiency

The CaO/fly ash sorbent was used to investigate the effects of impinging streams on the desulfurization efficiency. The desulfurization efficiencies at Ca/S = 2.0 with and without IS are shown in Fig. 9. The average desulfurization efficiencies decreased from 83.5% to 72.8% after the impinging streams were introduced. The measurements of the desulfurization efficiencies at Ca/S = 1.0 were repeated to verify the experimental reproducibility. The results were similar with the average desulfurization efficiencies decreasing from 69.2% to 54.5% after the impinging streams were introduced. After all the experiments were finished to obtain sufficient bottom material for the subsequent calculations, the material at the reactor bottom was weighed to calculate the ratio of the bottom material to the supplied material. The ratio was 63.3% for the IS case and 35.1% for the non-IS case.

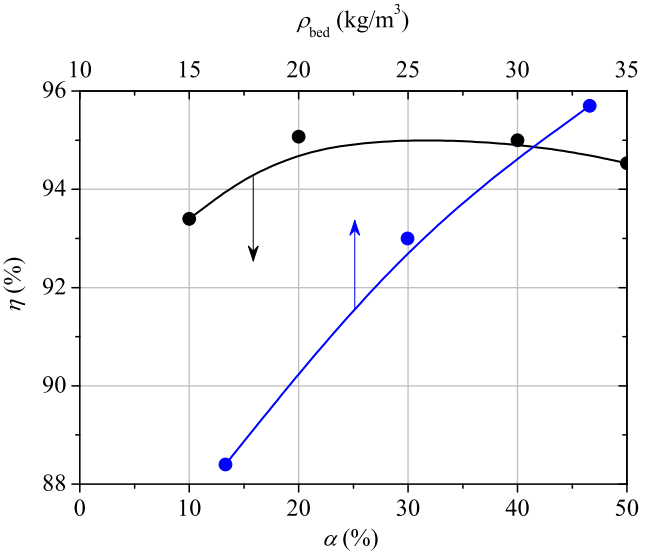

Fig. 8. Effects of the bed inventory and impinging stream ratio on the desulfurization efficiency in the IS-CFB reactor (ρ_{bed} = 33.3 kg/m^{2}s for the various α while α = 20% for the various ρ_{bed}).

Table 5
Effect of impinging particle material on the desulfurization efficiency (α = 20%).

Impinging particle material	U_{is} (m/s)	η (%)
Circulating spent sorbent	5.16	95.0
Circulating spent sorbent	15.25	93.4
Fresh sorbent	15.25	92.9

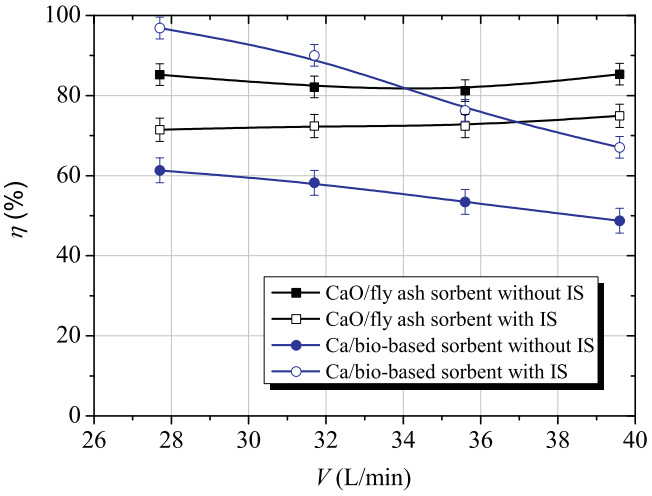

Fig. 9. Effect of impinging streams on the desulfurization efficiency for the two sorbents (T = 750 °C, Ca/S = 2.0).

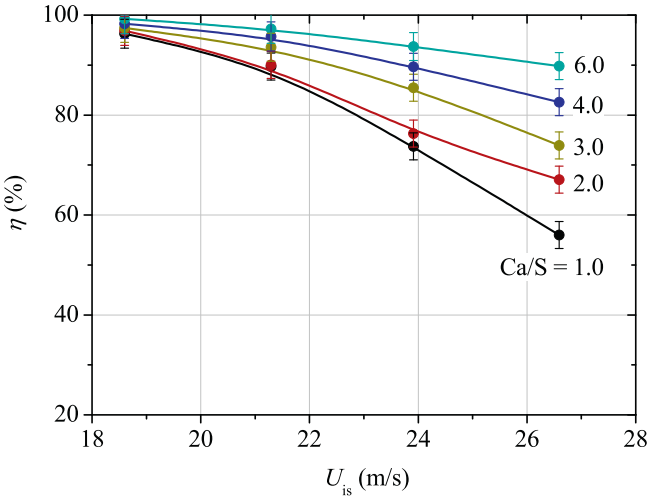

Fig. 10. Effect of the impinging velocity on the desulfurization efficiency for the Ca/bio-based sorbent (T = 750 °C).

The results show that the CaO/fly ash sorbent, which is large and dense, cannot be effectively entrained by the impinging streams, thus large amounts of sorbent drop to the reactor bottom. The CaO/fly ash sorbent is relatively dense, so the gas velocity is too small to entrain the sorbent particles. The bed superficial gas velocity was 2.5 m/s in the concept IS-CFB reactor, and ranged from 0.75 m/s to 1.07 m/s in the IS reactor. The desulfurization efficiency in the concept IS-CFB reactor is higher than in the small IS reactor for two main reasons. First, the residence time for the reactive gas is about 2.2 s in the 5.5 m long IS-CFB reactor, but is less than 0.8 s in the 0.6 m long IS reactor. Secondly, even though the inlet Ca/S ratios are equal for the two reactors, the actual Ca/S ratio in the IS-CFB reactor is much higher than in the IS reactor since a large amount of spent sorbent stays in the IS-CFB reactor.

The desulfurization efficiency is also dependent on the size of the impingement zone relative to the reactor length and volume. The effective SO_2 capture zone is longer in the IS-CFB reactor than in the CFB reactor as shown in Fig. 5, so the 0.6 m length is not long enough for the particles to react with the reactive gas. Previous studies showed that the desulfurization efficiency decreases as the impinging distance decreases in the range tested here and that there is an optimal ratio of the impinging distance to the IS inlet diameter that gives the highest desulfurization efficiency for a given design [8,11].

The Ca/bio-based sorbent, which has small particles and a low specific density, was used to verify the effects of the impinging streams on the desulfurization efficiencies with the results for Ca/S = 2.0 shown in Fig. 9. Unlike for the CaO/fly ash sorbent, the average desulfurization efficiencies for the Ca/bio-based sorbent increased from 55.4% to 82.6% with the impinging streams. For Ca/S = 1.0, the results were similar with the average desulfurization efficiencies increasing from 46.0% to 78.9%. The inventory at the reactor bottom was significantly lower with the impinging streams as the gas flow carries many more sorbent particles and the gas–solid contact time increases. When the gas velocity is relatively low, sorbent particles need to be small and light to be carried by the impinging streams; however, when the gas velocity is relatively high, larger, heavier particles are desirable because they have more inertia to penetrate into the opposing stream so they initially oscillate and then spiral upwards leading to longer residence times in the impingement zone.

Experiments were also conducted using the Ca/bio-based sorbent in the pilot scale CFB reactor. The Ca/bio-based sorbent had lower desulfurization efficiencies than the CaO/fly ash sorbent, since the Ca/bio-based sorbent particles were smaller and less dense so they did not circulate as long in the fluidized bed, but flew out of the cyclone and were collected by a bag filter.

3.2.2. Residence time in the impingement zone

The effect of the impinging velocity on the desulfurization efficiency was investigated to estimate the residence time in the impingement zone for the Ca/bio-based sorbent particles. The tests used five Ca/S ratios (1.0, 2.0, 3.0, 4.0 and 6.0) with the results shown in Fig. 10. The desulfurization efficiency reached 96.3% at Ca/S = 1.0 and U_{is} = 18.60 m/s. Thus the IS reactor can give a high desulfurization efficiency in a relatively short time. The intensive particle collisions break the particles into pieces to expose more unreacted fresh surface to the reactive gas, which improves the gas–solid mass transfer [7,28]. As shown in Fig. 10, the desulfurization efficiency decreases as the impinging velocity increases. Large impinging velocities have two negative effects on the desulfurization efficiency by reducing the impingement zone temperature which further reduces the sorbent activity, by reducing the total gas–solid residence time in the furnace.

The material balance equation gives:

$$\eta = X \cdot \mathrm{Ca/S} \tag{10}$$

As shown in Fig. 4, the calcium conversion rate, X, and the reaction time, t, are linearly related for $X \leqslant 0.5$ in the rapid reaction stage (stage I); therefore, the desulfurization efficiency is linearly related to the reaction time. Fig. 10 shows that $X > 0.5$ for Ca/S = 1.0 while $X \leqslant 0.5$ for Ca/S = 2.0, 3.0, 4.0 and 6.0, so the latter four Ca/S ratios (2.0, 3.0, 4.0 and 6.0) are then used to calculate the desulfurization efficiencies. The four solid lines in Fig. 11 come from Fig. 10. The total gas–solid contact time includes the residence time in the upper furnace, t_f, and the residence time in the impingement zone, t_{is}. For a given furnace length, the residence time in the upper furnace decreases as the gas velocity increases, as shown in Table 2. If the furnace length could be changed, the residence times in the upper furnace could be made equal at the various gas velocities (or

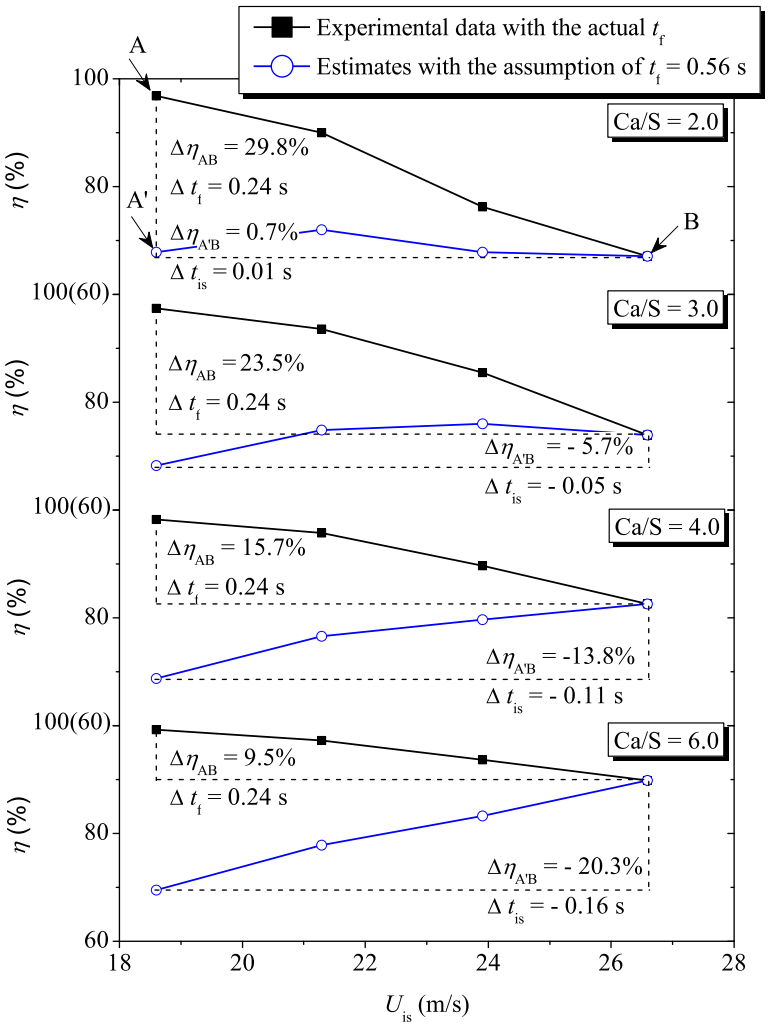

Fig. 11. Calculation of the residence time based on the experimental data (T = 750 °C).

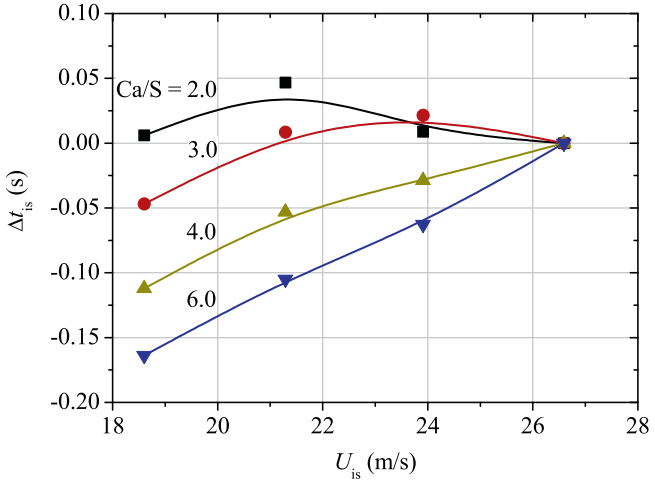

Fig. 12. Effect of the Ca/S ratio on the residence time for the Ca/bio-based sorbent (T = 750 °C).

impinging stream velocities). The desulfurization efficiencies could then be calculated as indicated below. The calculated results are shown as the hollow symbols in Fig. 11. For convenience, Ca/S = 2.0 will be used as an example with the symbols A, A′, and B denoting different points in Fig. 11. Taking t_f = 0.56 s as an example and setting the ratio of the desulfurization efficiencies to the residence times to be equal gives:

$$\frac{\eta_A}{t_{f,A}+t_{is,A}}=\frac{\eta_{A'}}{t_{f,A'}+t_{is,A'}}=\frac{\eta_B}{t_{f,B}+t_{is,B}} \tag{11}$$

$$t_{f,A'}=t_{f,B}=0.56\ \text{s} \tag{12}$$

$$t_{is,A'}=t_{is,A} \tag{13}$$

Defining $\Delta\eta_{AB}=\eta_A-\eta_B$ and $\Delta t_{AB}=t_A-t_B$, Eqs. (11)–(13) can be arranged to give:

$$\frac{\Delta\eta_{AB}}{\Delta t_{f,AB}+\Delta t_{is,AB}}=\frac{\Delta\eta_{A'B}}{\Delta t_{is,AB}} \tag{14}$$

$$\Delta t_{is,AB}=\frac{\Delta\eta_{A'B}}{\Delta\eta_{AB}-\Delta\eta_{A'B}}\cdot\Delta t_{f,AB} \tag{15}$$

The desulfurization efficiencies at A, A′ and B can be read from Fig. 11 and the residence times in the upper furnace can be obtained from Table 2. $\Delta\eta_{AB}$, $\Delta\eta_{A'B}$, and $\Delta t_{f,AB}$ in Eq. (15) are all known and $\Delta t_{is,AB}$ can then be calculated. For Ca/S = 2.0, as U_{is} increases from 18.60 m/s to 26.59 m/s, t_f decreases to 0.24 s, η decreases from 67.8% to 67.1%, and t_{is} increases by about 0.01 s. For Ca/S = 3.0, 4.0 and 6.0, the residence times in the impingement zone increase by 0.05, 0.11 and 0.16 s. This study assumes that the inlet temperature decrease can be neglected. The distance from the midlevel inlet to

the location where the temperature reaches 750 °C is 150 mm, which is 25% of the total 600 mm length. If all the temperatures in the furnace were reduced to the midlevel temperature, 630 °C, the desulfurization efficiency would be reduced by no more than 7% [18] and if the temperatures in this 150 mm region were reduced to 630 °C, the desulfurization efficiency would be reduced by no more than 2%.

The residence time for the other gas flow rates were also compared with the residence time for U_{is} = 26.59 m/s, with the time differences, Δt_{is}, shown in Fig. 12. For Ca/S = 2.0 and 3.0, the time differences first increase and then decrease as the gas velocity increases. These trends are consistent with Wu's description [7]; although the trends are not very obvious. For Ca/S = 4.0 and 6.0, the time differences clearly increase with the gas flow rate. The results show that the residence time is significantly influenced by the Ca/S ratio as well as the gas flow rate. For Ca/S = 2.0, 3.0, 4.0 and 6.0, the solid to gas mass ratios are calculated to be 0.93×10^{-2}, 1.39×10^{-2}, 1.85×10^{-2} and 2.78×10^{-2}. This ratio refers to the carried solid-particle mass per mass of gas. As the mass of solid particles carried by the gas increases, the particle residence time increases. For the CaO/fly ash sorbent, the solid to gas mass ratio is 3.24×10^{-2} for Ca/S = 2.0, so residence time is not improved by larger particle sizes.

The residence time in the impingement zone is less than 0.16 s in this study; however, it is a relatively large proportion of the gas–solid residence time in the upper furnace, which is 0.56–0.80 s. The residence time is smaller in this study than in other studies [7,12–14] since the residence time in the impingement zone is related to the reaction zone size as well as the operating conditions. Wu [7] showed that the gas–solid residence time in the impingement zone initially increases and then decreases with increasing impinging stream velocity. Thus, an appropriate impinging velocity will give an optimal residence time. However, a very large impinging velocity will increase the energy consumption and result in a short gas–solid residence time in the upper furnace. If this effect is greater than the effect of the gas–solid residence time in the impingement zone, then the impinging velocity should not be increased.

4. Conclusions

The numerical simulation results indicate that the introduction of impinging streams to the CFB reactor significantly improves the desulfurization efficiency from 89.5% to 95.1%. Different from the conventional CFB reactor, the IS-CFB reactor makes the radial particle volume fraction distribution in the cross section more homogeneous and the effective SO_2 capture zone much larger. The lateral gas flow in the impingement zone intensifies the gas–solid mass transfer. The IS-CFB reactor gives a much higher desulfurization efficiency with a much lower bed pressure drop than the CFB reactor. The spent sorbent can be fully used in the IS-CFB reactor. The desulfurization efficiency in a large IS-CFB reactor is higher than in a small IS reactor due to a longer gas–solid residence time and a higher actual Ca/S ratio in the large reactor.

Experimental results show that the Ca/bio-based sorbent gives higher desulfurization efficiencies than the CaO/fly ash sorbent, for the latter which is large and dense cannot be effectively entrained by the impinging streams. When the gas velocity is relatively low, sorbent particles need to be small and light to be carried by the impinging streams. A method for combining experiments and calculations is developed to estimate the gas–solid residence time in the impingement zone, and the residence time was found to increase by about 0.16 s for the Ca/bio-based sorbent in this work. The results show that the residence time is significantly influenced not only by the gas velocity but also by the solid to gas mass ratio.

Acknowledgement

This work was supported by the National Basic Research Program of China (973 Program) No. 2006CB200305.

References

[1] Y.Z. Li, H.L. Tong, Y.Q. Zhuo, Y. Li, X.C. Xu, Simultaneous removal of SO_2 and trace As_2O_3 from flue gas: mechanism, kinetics study and effect of main gases on arsenic capture, Environ. Sci. Technol. 41 (2007) 2894–2900.
[2] J. Zhang, C.F. You, C.H. Chen, Effect of internal structure on flue gas desulfurization with rapidly hydrated sorbent in a circulating fluidized bed at moderate temperatures, Ind. Eng. Chem. Res. 49 (2010) 11464–11470.
[3] J. Zhang, C.F. You, C.H. Chen, H.Y. Qi, X.C. Xu, Effect of near-wall air curtain on the wall deposition of droplets in a semidry flue gas desulfurization reactor, Environ. Sci. Technol. 41 (2007) 4415–4421.
[4] D.R. Bai, J.X. Zhu, Y. Jin, Z.Q. Yu, Internal recirculation flow structure in vertical upflow gas-solids suspensions Part I. A core-annulus model, Powder Technol. 85 (1995) 171–177.
[5] A. Tamir, Impinging Stream Reactors Fundamentals and Applications, Elsevier, Amsterdam, 1994.
[6] C. Srisamran, S. Devahastin, Numerical simulation of flow and mixing behavior of impinging streams of shear-thinning fluids, Chem. Eng. Sci. 61 (2006) 4884–4892.
[7] Y. Wu, Impinging Streams Fundamentals, Properties, and Applications, Elsevier, Amsterdam, 2007.
[8] W.Z. Jiao, Y.Z. Liu, G.S. Qi, A new impinging stream-rotating packed bed reactor for improvement of micromixing iodide and iodate, Chem. Eng. J. 157 (2010) 168–173.
[9] Y. Berman, A. Tanklevsky, Y. Oren, A. Tamir, Modeling and experimental studies of SO_2 absorption in coaxial cylinders with impinging streams: Part I, Chem. Eng. Sci. 55 (2000) 1009–1021.
[10] Y. Berman, A. Tanklevsky, Y. Oren, A. Tamir, Modeling and experimental studies of SO_2 absorption in coaxial cylinders with impinging streams: Part II, Chem. Eng. Sci. 55 (2000) 1023–1028.
[11] Y. Wu, Q. Li, F. Li, Desulfurization in the gas-continuous impinging stream gas-liquid reactor, Chem. Eng. Sci. 62 (2007) 1814–1824.
[12] K. Luzzatto, A. Tamir, I. Elperin, A new two-impinging streams heterogeneous reactor, AIChE J. 30 (1984) 600–608.
[13] E. Rajaie, M. Sohrabi, Application of the Monte Carlo technique in simulation of flow and modeling the residence time distribution in a continuous two impinging liquid–liquid streams contactor, Chem. Eng. J. 143 (2008) 249–256.
[14] M. Du, C.S. Zhao, B. Zhou, H.W. Guo, Y.L. Hao, A modified DSMC method for simulating gas-particle two-phase impinging streams, Chem. Eng. Sci. 66 (2011) 4922–4931.
[15] C.S. Ho, S.M. Shih, $Ca(OH)_2$/fly ash sorbents for SO_2 removal, Ind. Eng. Chem. Res. 31 (1992) 1130–1135.
[16] A. Garea, I. Fernández, J.R. Viguri, M.I. Ortiz, J. Fernández, M.J. Renedo, J.A. Irabien, Fly-ash/calcium hydroxide mixture for SO_2 removal: structure properties and maximum yield, Chem. Eng. J. 66 (1997) 171–179.
[17] C.F. Liu, S.M. Shih, R.B. Lin, Effect of $Ca(OH)_2$/fly ash weight ratio on the kinetics of the reaction of $Ca(OH)_2$/fly ash sorbents with SO_2 at low temperatures, Chem. Eng. Sci. 59 (2004) 4653–4655.
[18] Y.R. Li, H.Y. Qi, C.F. You, L.Z. Yang, Comprehensive sulfation model verified for T–T sorbent clusters during flue gas desulfurization at moderate temperatures, Fuel 89 (2010) 2081–2087.
[19] Y.R. Li, H.Y. Qi, J. Wang, SO_2 Capture and attrition characteristics of a CaO/bio-based sorbent, Fuel 93 (2012) 258–263.
[20] H.S. Shang, F. Yang, Y. Kou, Reparation and desulfurization of Na_2CO_3/straw sorbents for removing SO_2 from flue gas, Environ. Sci. 24 (2003) 68–73.
[21] B. Hou, H.Y. Qi, C.F. You, X.C. Xu, Dry desulfurization in a circulating fluidized bed (CFB) with chain reactions at moderate temperatures, Energ. Fuel. 19 (2005) 73–78.
[22] F. Li, Investigations on the turbulent gas-solid two-phase interactions in fluidized desulfurization process, Ph.D. Dissertation, Tsinghua University, Beijing, 2009 (in Chinese).
[23] H.Y. Qi, Euler/Euler Simulation der Fluiddynamik zirkulierender Wirbelschichten, Verlag Mainz, Wissenschaftsverlag, Aachen, 1997.
[24] W. Wang, J.H. Li, Simulation of gas-solid two-phase flow by a multi-scale CFD approach—extension of the EMMS model to the sub-grid level, Chem. Eng. Sci. 62 (2007) 208–231.
[25] D. Gidaspow, Multiphase flow and fluidization: continuum and kinetic theory descriptions, Academic Press, Boston, 1994.
[26] C. Chen, F. Li, H.Y. Qi, Modeling of the flue gas desulfurization in a CFB riser using the Eulerian approach with heterogeneous drag coefficient, Chem. Eng. Sci. 69 (2012) 659–668.
[27] A.J. Yan, J.H. Pärssinen, J.X. Zhu, Flow properties in the entrance and exit regions of a high-flux circulating fluidized bed riser, Powder Technol. 131 (2003) 256–263.
[28] S.J. Royaee, M. Sohrabi, Application of photo-impinging streams reactor in degradation of phenol in aqueous phase, Desalination 253 (2010) 57–61.